



## High-Performance Low-Voltage Tetracene Phototransistors with Polymer/ $\text{AlO}_x$ Bilayer Dielectric

Jeong-M. Choi,<sup>a</sup> Kimoon Lee,<sup>a</sup> D. K. Hwang,<sup>a</sup> Ji Hoon Park,<sup>b</sup> Eugene Kim,<sup>b</sup> and Seongil Im<sup>a,z</sup>

<sup>a</sup>Institute of Physics and Applied Physics, Yonsei University, Seoul 120-749, Korea

<sup>b</sup>Department of Information and Display, Hongik University, Seoul 121-791, Korea

We report on the tetracene-based photo thin-film transistors (photo-TFTs) which adopt thin poly-4-vinylphenol (PVP)/aluminum oxide ( $\text{AlO}_x$ ) bilayer and semitransparent  $\text{NiO}_x$  for a gate dielectric and source/drain (S/D) electrode, respectively. Quite a large capacitance of  $31 \text{ nF/cm}^2$  was effectively achieved from the thin polymer/high- $k$  oxide dielectric bilayer that also showed a high dielectric strength of  $\sim 4 \text{ MV/cm}$ . Our tetracene-based TFTs exhibited quite a good field effect mobility ( $\sim 0.23 \text{ cm}^2/\text{V s}$ ) and a high on/off current ratio of  $\sim 10^5$ , while operating at a voltage less than  $-8 \text{ V}$ . The tetracene-TFTs demonstrated good static photoresponses to green (540 nm), blue (450 nm), and ultraviolet (364 nm) illuminations under the low voltage.  
© 2006 The Electrochemical Society. [DOI: 10.1149/1.2211847] All rights reserved.

Manuscript submitted March 23, 2006; revised manuscript received May 4, 2006. Available electronically June 26, 2006.

Organic thin-film transistors (OTFTs) have been extensively studied due to their potentials toward driving circuit for display or low-cost logic applications.<sup>1-4</sup> Among many types of OTFTs, pentacene-based transistors have been the most promising in terms of field mobility. Tetracene-based TFT, where its active layer has the highest occupied molecular orbital-lowest unoccupied molecular orbital (HOMO-LUMO) gap of  $\sim 2.3 \text{ eV}$ , does not have a high field mobility compared to those of pentacene-based TFTs, always yielding an order of magnitude lower value. Therefore they have not been the focus of the present organic electronics research that prefers fast charge transport or fast switching, and thus only a few studies on tetracene-TFTs have been reported.<sup>5-8</sup> However, tetracene-based TFTs and tetracene films should still be in high demand within the framework of optoelectronics, for example, as light-emitting transistors<sup>6-8</sup> and light-emitting diodes.<sup>9</sup> Photodetectors and photovoltaic cells are also fascinating forms of devices, being able to take the tetracene films for active components as recently reported.<sup>10</sup> Because pentacene-based devices cannot carry out any photo- or optoelectronic missions despite their excellent dark electronic properties,<sup>10</sup> studies on achieving a high-quality tetracene TFT with an enhanced field mobility and a low operating voltage should be very important for advanced optoelectronic applications. In the present study, we have fabricated low-voltage, high performance tetracene-based photo-TFTs, adopting a thin poly-4-vinylphenol (PVP)/aluminum oxide ( $\text{AlO}_x$ ) bilayer for a gate dielectric and semitransparent  $\text{NiO}_x$  for source/drain (S/D) electrodes.

### Experimental

Prior to  $\text{AlO}_x$  film deposition on indium-tin-oxide (ITO) glass, the glass was cleaned with acetone, ethanol, and deionized water in that order. After that, the 100 nm thick  $\text{AlO}_x$  films were deposited on the ITO glass by radio-frequency (rf) magnetron sputtering in a vacuum chamber at room temperature (the initial base pressure was about  $2 \times 10^{-6}$  Torr and the working Ar pressure was fixed at 20 mTorr). The thickness and sheet resistance of the ITO films were 79 nm and  $30 \Omega/\square$ , respectively. PVP films on the  $\text{AlO}_x$  layer were then prepared to a thickness of 45 nm from solutions of PVP and poly (melamine-co-formaldehyde), as a cross-linking agent in propylene glycol monomethyl ether acetate (PGMEA), by spin coating and subsequent cross-linking (curing) at  $175^\circ\text{C}$  for 1 h in a vacuum oven. Then, tetracene channels and S/D electrodes ( $\text{NiO}_x$ ) were sequentially patterned on the  $\text{AlO}_x$  layer with shadow masks by thermal evaporation. The deposition rate was fixed to 0.1 nm/s for the evaporation of tetracene (Aldrich Chem. Co.,  $\sim 98\%$  purity), and was controlled to be 3 nm/s for the evaporation of  $\text{NiO}$  (99.97%

purity). The thicknesses of tetracene and  $\text{NiO}_x$  films were 50 and 100 nm, respectively. The sheet resistance of  $\text{NiO}_x$  films was determined to be  $60 \sim 100 \Omega/\square$  by Hall measurements. Figure 1a shows the schematic cross section of our TFT with a nominal channel length,  $L$  of  $90 \mu\text{m}$  (width,  $W = 500 \mu\text{m}$ ). The surface image of our tetracene channel was observed with atomic force microscopy (AFM, SPM IV, Digital Instrument).

All electrical and photoelectric characterizations were carried out with a semiconductor parameter analyzer (model HP 4155C, Agilent Technologies) and capacitance-voltage (C-V) measurements were made with a HP4284 capacitance meter (1 MHz). Green (540 nm), blue (450 nm), and ultraviolet (UV, 364 nm) lights were illuminated on our TFT by a light source (Oriol Optical System) consisting of a

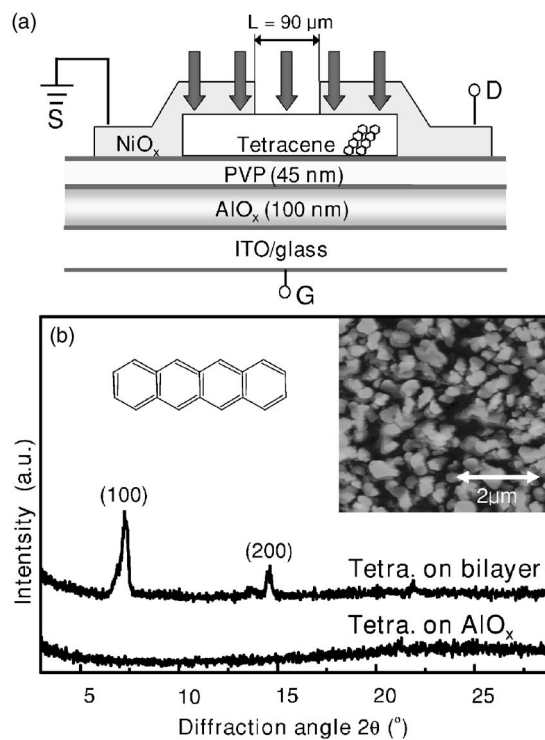


**Figure 1.** (a) Schematic cross section of our tetracene-based TFT with the hybrid bilayer dielectric and semitransparent  $\text{NiO}_x$  (see the light penetrate the  $\text{NiO}_x$  S/D area in the scheme). (b) XRD patterns of tetracene films deposited on PVP/ $\text{AlO}_x$ /ITO glass and  $\text{AlO}_x$ /ITO glass substrates. The insets show the molecular structure of tetracene (left) and the AFM surface image of our tetracene film thermally deposited on the PVP/ $\text{AlO}_x$ /ITO glass (right).

<sup>z</sup> E-mail address: semicon@yonsei.ac.kr

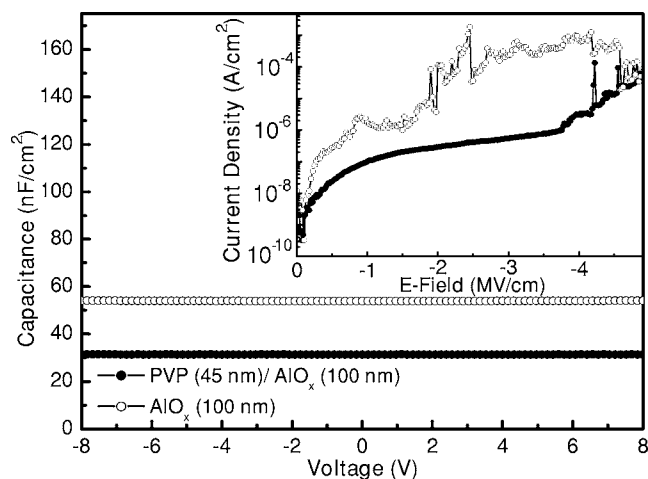


**Figure 2.** 1 MHz C-V characteristics measured from PVP/ $\text{AlO}_x$  bilayer and single  $\text{AlO}_x$  dielectric films. Inset: current density vs electric field curves of both dielectrics.

500 W Hg (Xe) arc lamp and a monochromator covering the wavelength in the range of 350–700 nm. The optical power of the incident monochromatic light was measured by a UV-enhanced Si detector (Advantest TQ 8210) and in the present study the optical power density of 364 nm UV was fixed to  $\sim 0.64 \text{ mW/cm}^2$ , while those of the other visible lights were  $\sim 0.1 \text{ mW/cm}^2$ .

### Results and Discussion

Figure 1a presents the cross section of device structure where tetracene was employed as the active layer formed on the PVP/ $\text{AlO}_x$  bilayer dielectric. Through this organic-inorganic hybrid or bilayer approach we tried to gain the following three advantages: changing the state of the top dielectric surface from rough hydrophilic inorganic to smooth hydrophobic organic, maintaining high dielectric capacitance with a thin inorganic oxide, and, finally, improving the overall dielectric strength or reducing the gate current leakage. In Fig. 1b, the X-ray diffraction (XRD) results from a tetracene film grown on PVP/ $\text{AlO}_x$ /ITO glass and another film grown on  $\text{AlO}_x$ /ITO glass substrates are shown. While the tetracene film deposited on the bare  $\text{AlO}_x$  layer shows no diffraction peaks, the film deposited on the PVP/ $\text{AlO}_x$  bilayer displays good crystalline ordering because the top smooth PVP layer was in a hydrophobic state, known to help organic molecules remain crystalline during deposition.<sup>11</sup> The inset of Fig. 1b shows AFM image of our tetracene active layer grown on the bilayer surface. The image is not much dendritic compared to that of a usual crystalline pentacene film, but it is very comparable to the previously reported images of well-grown tetracene films.<sup>12</sup>

Figure 2 displays the C-V and current density vs electric field ( $J$ - $E$ ) relationships of single 100 nm thick  $\text{AlO}_x$  and bilayer PVP (45 nm)/ $\text{AlO}_x$  (100 nm) films deposited on ITO glass substrates (we deposited 300  $\mu\text{m}$  diam Au dots on top for these measurements). As shown in Fig. 2, the dielectric capacitances ( $C_{\text{AlO}_x}$  and  $C_{\text{bilayer}}$ ) of the single  $\text{AlO}_x$  layer and PVP/ $\text{AlO}_x$  bilayer films were measured to be about 54 and 31  $\text{nF/cm}^2$ , respectively. Because the dielectric constants of PVP and  $\text{AlO}_x$  were reported to be  $\sim 3.7$  and  $\sim 6$ , respectively,<sup>13,14</sup> the measured capacitance values are quite reliable. According to the  $J$ - $E$  results in the inset of Fig. 2, it is also noted that our bilayer dielectric approach is quite effective in the aspects of dielectric strength and leakage current. Compared to the single  $\text{AlO}_x$  layer, our bilayer dielectric with 45 nm thick PVP on top showed much improved leakage current resistance (the dielectric strength was about 4 MV/cm in our leakage standard of  $1 \times 10^{-6} \text{ A/cm}^2$ ). Combining the results from Fig. 1b and the inset in Fig. 2, we regarded that using our bilayer dielectric, instead of using

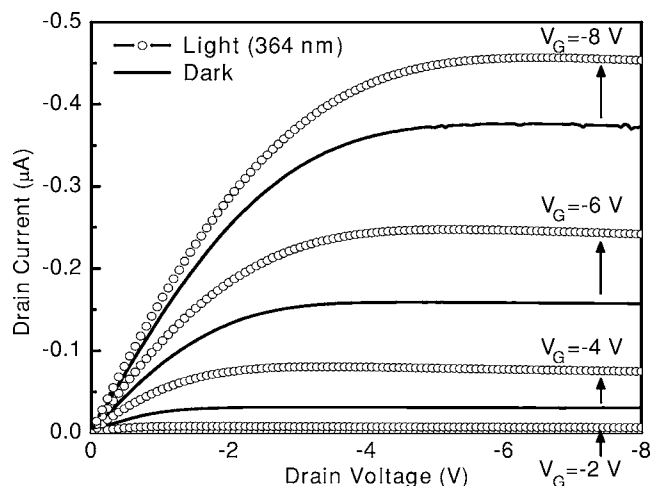


**Figure 3.** The drain current-drain voltage ( $I_D$ - $V_D$ ) characteristics of tetracene TFT with the bilayer dielectric and  $\text{NiO}_x$  S/D electrode. Photoelectric effects were also observed under UV (364 nm) lights of  $0.64 \text{ mW/cm}^2$ .

the single high- $k$   $\text{AlO}_x$  layer, could be an optimum way to fabricate good tetracene-TFTs.

The drain current-drain voltage ( $I_D$ - $V_D$ ) characteristics of tetracene-based TFTs with the bilayer dielectric and  $\text{NiO}_x$  S/D electrodes are shown in Fig. 3. Under a gate bias ( $V_G$ ) of  $-8 \text{ V}$  our TFT employing a  $\text{NiO}_x$  S/D electrode, instead of a usual electrode such as Au, displays the saturation current of  $0.36 \mu\text{A}$ . We previously reported our thermally evaporated conducting  $\text{NiO}_x$  to be quite off-stoichiometric (Ni-rich) and to have a larger work function than that of Au by  $\sim 0.2 \text{ eV}$ .<sup>15</sup> It is thus expected that employing conducting  $\text{NiO}_x$  may lower the contact resistance between electrode and tetracene channel. The  $I_D$  was increased to  $0.46 \mu\text{A}$  by UV illumination (364 nm) because our tetracene channel with the HOMO-LUMO gap of 2.3 eV must have experienced photoabsorption and photoelectric effects.<sup>10</sup>

Drain current-gate bias ( $I_D$ - $V_G$ ) relationships were also obtained from our tetracene-based TFTs with  $\text{NiO}_x$  electrodes at a certain drain-source voltage,  $V_{DS} = -6 \text{ V}$  as shown in the  $\sqrt{-I_D}$  vs  $V_G$  (Fig. 4a) and the  $\log(-I_D)$  vs  $V_G$  curves (Fig. 4b). Our tetracene OTFT with the  $\text{NiO}_x$  electrode showed a high mobility of  $0.23 \text{ cm}^2/\text{V s}$  (saturation regime) and a high on/off current ratio of  $\sim 10^5$ . According to Fig. 4a, the threshold voltage ( $V_T$ ) is estimated to be  $-3.5 \text{ V}$  which is low enough for turning on a TFT. Such a low voltage operation of tetracene-TFT has not been reported yet (to the best of our knowledge). These low-voltage high-mobility performances mainly ascribe to the bilayer dielectric approach that enables good-crystalline tetracene growth and simultaneously quite a high dielectric charging at the channel/PVP interface, being partially owing to the incorporation of  $\text{NiO}_x$  electrode in our device.

Our tetracene-TFTs with  $\text{NiO}_x$  responded sensitively to the light, turned on by UV light (364 nm, 3.4 eV with an optical power density of  $0.64 \text{ mW/cm}^2$ ) at a lower gate voltage of  $-1.2 \text{ V}$  (see Fig. 4a and find more details on the turn-on voltage shift elsewhere<sup>10</sup>). The photo-to-dark current ratio ( $I_{\text{ph}}/I_{\text{dark}}$ ) for tetracene-based TFTs was  $\sim 10^4$  as  $I_{\text{dark}}$  found at  $V_G = -2 \text{ V}$  was regarded as the minimum current. The semi-transparent  $\text{NiO}_x$  S/D electrode could also be used as a photon window as it has been reported to have an optical energy gap of  $\sim 4.1 \text{ eV}$  and a visible-range transmittance of  $\sim 30\%$ .<sup>14</sup> Hence, our tetracene TFT with the semitransparent conductive oxide electrode effectively responded to the green (540 nm, 2.3 eV) and blue (450 nm, 2.76 eV) lights, which were much weaker than UV in intensity (the optical power density of the visible lights was  $\sim 0.1 \text{ mW/cm}^2$ ). About 30% of initial visible photons (but 10% for the 364 nm UV)<sup>14</sup> would penetrate our S/D window area to excite

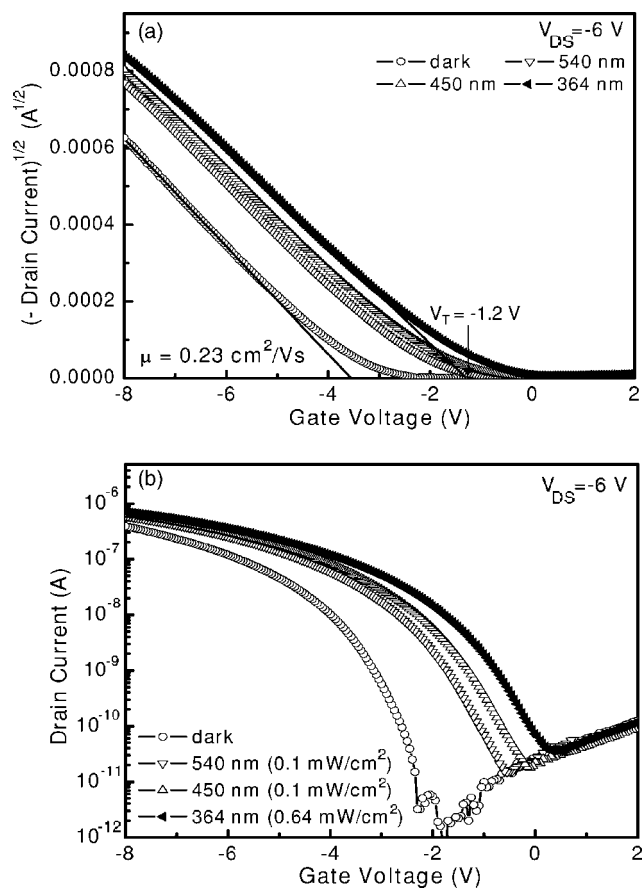


**Figure 4.** (a)  $\sqrt{-I_D}$  vs  $V_G$  and (b)  $\text{Log}(-I_D)$  vs  $V_G$  curves obtained from our tetracene-based photo-TFT at  $V_{DS} = -6$  V. Our tetracene-based TFT with semitransparent  $\text{NiO}_x$  S/D was illuminated by green (540 nm,  $0.1 \text{ mW/cm}^2$ ), blue (450 nm,  $0.1 \text{ mW/cm}^2$ ), and UV (364 nm,  $0.64 \text{ mW/cm}^2$ ) lights.

the depleted tetracene below as well as an open channel area which was not covered by S/D electrode (see Fig. 1a). Therefore, our tetracene TFT using the bilayer dielectric and the  $\text{NiO}_x$  S/D could be an advanced model of organic photo-TFTs operating at the low voltage of  $-8$  V.

## Conclusions

In summary, we have fabricated tetracene-based photo-TFTs with thin PVP/ $\text{AlO}_x$  bilayer dielectric and semitransparent  $\text{NiO}_x$  S/D electrode. A large capacitance of  $31 \text{ nF/cm}^2$  and a high dielectric strength of  $\sim 4 \text{ MV/cm}$  were achieved from the thin polymer/high- $k$  oxide dielectric film. Our tetracene-based TFTs exhibited quite a high field effect mobility ( $\sim 0.23 \text{ cm}^2/\text{V s}$ ) and a high on/off current ratio of  $\sim 10^5$  while operating at less than  $-8$  V. The tetracene-TFTs also demonstrated good static photoresponses to green (540 nm), blue (450 nm), and ultraviolet (364 nm) illuminations, showing a large  $I_{ph}/I_{dark}$  of  $\sim 10^4$  for UV. We conclude that our tetracene-based TFT jointly adopting semitransparent  $\text{NiO}_x$  for the S/D electrodes and a PVP/ $\text{AlO}_x$  bilayer for a gate dielectric is an advanced form of low-voltage organic photo-TFTs.

## Acknowledgments

This research was performed with the financial support from KOSEF (program no. M1-0214-00-0228) and LG. Philips LCD (project year 2005). We also acknowledge the support from Brain Korea 21 Project.

Yonsei University assisted in meeting the publication costs of this article.

## References

1. C. D. Dimitrakopoulos and P. R. L. Malenfant, *Adv. Mater. (Weinheim, Ger.)*, **14**, 99 (2002).
2. F. Eder, H. Klauk, M. Halik, U. Zschieschang, G. Schmid, and C. Dehm, *Appl. Phys. Lett.*, **84**, 2673 (2004).
3. L.-L. Chua, R. H. Friend, and P. K. H. Ho, *Appl. Phys. Lett.*, **87**, 253512 (2005).
4. H. E. A. Huitema, G. H. Gelinck, J. B. P. H. van der Putten, K. E. Kuijk, C. M. Hart, E. Cantatore, P. T. Herwig, A. J. J. M. van Breemen, and D. M. de Leeuw, *Nature (London)*, **414**, 599 (2001).
5. D. J. Gundlach, J. A. Nichols, L. Zhou, and T. N. Jackson, *Appl. Phys. Lett.*, **80**, 2925 (2002).
6. A. Hepp, H. Heil, W. Weise, M. Ahles, R. Schmechel, and H. V. Seggern, *Phys. Rev. Lett.*, **91**, 157406 (2003).
7. C. Santato, I. Manunza, A. Bonfiglio, F. Cicoira, P. Cosseddu, R. Zamboni, and M. Muccini, *Appl. Phys. Lett.*, **86**, 141106 (2005).
8. J. Reynaert, D. Cheyns, D. Janssen, R. Müller, V. I. Arkhipov, J. Genoe, G. Borghs, and P. Heremans, *J. Appl. Phys.*, **97**, 114501 (2005).
9. E.-A. You, Y.-G. Ha, Y.-S. Choi, and J.-H. Choi, *Synth. Met.*, **153**, 209 (2005).
10. J.-M. Choi, J. Lee, D. K. Hwang, J. H. Kim, S. Im, and E. Kim, *Appl. Phys. Lett.*, **88**, 043508 (2006).
11. H. Klauk, M. Halik, U. Zschieschang, G. Schmid, W. Radlik, and W. Weber, *J. Appl. Phys.*, **92**, 5259 (2002).
12. F. Cicoira, C. Santato, F. Dinelli, M. Murgia, M. A. Loi, F. Biscarini, R. Zamboni, P. Heremans, and M. Muccini, *Adv. Funct. Mater.*, **15**, 375 (2005).
13. D. K. Hwang, J. H. Park, J. Lee, J.-M. Choi, J. H. Kim, E. Kim, and S. Im, *J. Electrochem. Soc.*, **153**, G23 (2006).
14. J.-M. Choi, D. K. Hwang, J. H. Kim, and S. Im, *Appl. Phys. Lett.*, **86**, 123505 (2005).
15. K. Lee, J. H. Kim, and S. Im, *Appl. Phys. Lett.*, **88**, 023504 (2006).